Accuracy improvement by means of porosity assessment and standards optimization in SEM-EDS and XRF elemental analyses on archaeological and historical pottery and porcelain

ACCURACY IMPROVEMENT BY MEANS OF POROSITY ASSESSMENT AND STANDARDS OPTIMIZATION IN SEM-EDS AND XRF ELEMENTAL ANALYSES ON ARCHAEOLOGICAL AND HISTORICAL POTTERY AND PORCELAIN

F. Turco*, P. Davit, R. Cossio, A. Agostino, L. Operti

* francesca.turco@unito.it

Journal of Archaeological Science: Reports

Volume 12, April 2017, Pages 54–65

http://dx.doi.org/10.1016/j.jasrep.2017.01.022

ACCURACY IMPROVEMENT BY MEANS OF POROSITY ASSESSMENT AND STANDARDS OPTIMIZATION IN SEM-EDS AND XRF ELEMENTAL ANALYSES ON ARCHAEOLOGICAL AND HISTORICAL POTTERY AND PORCELAIN

F. Turco[*,1], P. Davit[1,2], R. Cossio[3,2], A. Agostino[1,2], L. Operti[1,2]

[1] Department of Chemistry, Università di Torino, Via Pietro Giuria 7, 10125, Torino, Italy.

[2] NIS Centre of Excellence, Via Pietro Giuria 7, 10125, Torino, Italy.

[3] Department of Earth Science, Università di Torino, Via Valperga Caluso 35, 10125, Torino, Italy

* Corresponding author. Tel.: +39 011 6707583; fax: +39 011 2367583; *E-mail address*: francesca.turco@unito.it

ABSTRACT

SEM-EDS and XRF analyses of pellets produced with powdery clay and ceramic standards and fired at increasing temperatures showed a systematic overestimation of the abundance of heavier detected elements (K, Ca, Ti and Fe) using the conventional procedure of calibration with massive mineral/glass certified materials followed by normalization of the detected values. Errors were particularly noticeable for samples fired in the typical range of temperatures of archaeological and historical pottery (600-900 °C) and for unfired samples, and were attributed to material porosity. An extremely simple method based on the SEM-BSE image analysis is proposed for the semi-quantitative evaluation of porosity. A remarkable increase of accuracy, especially for SEM-EDS, was evidenced when the calibration is performed using a standard with porosity comparable to the samples, with regard to the pottery temperature range. Conversely, for the analysis of high-fired samples simulating porcelain (1200 °C) no substantial difference was observed with respect to the usual massive minerals/glass calibration. Finally, results showed the unsuitability of calibration performed by means of unfired pellets, for both pottery and porcelains.

Keywords: X-ray elemental techniques, SEM-EDS, Calibration, Accuracy, Ceramic materials.

1. INTRODUCTION

Energy Dispersive X-ray Spectrometry coupled with Scanning Electron Microscopy (SEM-EDS) and X-Ray Fluorescence (XRF) Spectrometry are widely used methods for the (archaeometric) determination of major and minor elements in pottery and porcelain (Casadio and Bezur, 2009; Freestone et al., 2003; Mirti, 2000; Musílek et al., 2012; Özçatal et al., 2014; Tite et al., 2015; Tite, 2008; Tite and Bimson, 1991).

The choice and the procedure of obtaining the appropriate standards for instruments calibration for this kind of samples are not trivial. As a general rule, SEM-EDS and XRF calibrations are performed by using standards as similar as possible to the materials to be analyzed (Goldstein et al., 1992; Liritzis et al., 2011; Newbury and Ritchie, 2013; Shackley, 2011). In the case of pottery and porcelain the choice is quite awkward due to the scarceness of suitable commercial standards, moreover usually in the form of powder. The XRF standard calibration procedure generally prescribes the use of glass (or fused disk) standards, or pressed pellets (Shackley, 2011). In the specific case of pottery and porcelain analyses standards prepared from clay or ceramic powdery certified materials are often utilized as calibration standards (Papageorgiou and Liritzis, 2007; Turco et al., 2015; Yan et al., 2015). As for SEM-EDS, massive minerals and oxides standards are usually employed for calibration (Davit et al., 2014; Mirti and Davit, 2001; Montana et al., 2013; Seetha and Velraj, 2015; Yin et al., 2011). However, the instrumental response is influenced by the intrinsic characteristics of the matrix, in the case of ceramic and porcelain materials strongly depending on the temperature and atmosphere of the firing step, impacting both on the mineralogical composition and on the morphology, i.e. degree of sintering and/or vitrification, absence and/or presence of voids, cracks and bubbles, that is to say on the consequent porosity (Maniatis and Tite, 1981). Indeed, since SEM-EDS requires solid, flat-polished specimens (Goldstein et al., 1992), the use of this technique in the analysis of ceramic or porcelain objects, is not trivial.

First of all the oxides weight % total concentration (indicated below as "analytical total") is usually quite different from the expected value of 100% and a normalization of the values is the usual procedure (Freestone, 1982; Ting et al., 2015). The reason for the low analytical totals is that in most cases the electron path length in the material is higher than in the case of a non-porous material causing an even more serious problem since the fraction of detected X-rays varies as a function of this path and of the energy of the specific X-ray. The lower the energy of the analyzed X-ray line, the higher the absorption (Knížek and Jurek, 1994): for this reason, remarkable attention must be placed when massive mineral and oxides standards are used for SEM-EDS calibration of porous materials with a chemical composition ranging over a broad interval of atomic masses, as in the case of pottery and porcelain. In the case of XRF, the problem of the path length is fortunately less essential, but it is still significant for light elements, due to the low path escape of their signals. Moreover, being equal the signal source region, the medium density of the material is lower than expected and noticeable errors might be caused when the correction algorithm is applied.

To individuate the more suitable standard preparation method for SEM-EDS and XRF calibration in the case of pottery and porcelain analyses, two commercial Standard/Certified Reference Materials (SRM/CRM), a clay and a ceramic powder, were subjected to different preparation procedures and to firing at diverse temperatures to obtain series of simulated samples. Moreover, a semi-quantitative evaluation of the porosity of these materials was carried out to correlate these results with the compositional data obtained by SEM-EDS and XRF analyses. Finally, the ceramic standard samples were used as calibration standards in the analyses of the clay standard samples, in order to identify the most appropriate standard choice with respect to samples fired at different temperatures.

2. MATERIALS AND METHODS

2.1 Samples

The Standard Reference Material SRM 98b (dried and powdered plastic clay) from the National Institute of Standards and Technology (NIST, Gaithersburg, MD, USA) and the Certified Reference Material SARM 69 (powdered ceramic from Iron Age potsherds) from MINTEK (Johannesburg, SA) were compressed with a hydraulic press under a pressure of 12 tons in order to obtain 1 cm diameter and 2 mm thickness pellets. Four pellets for each material were prepared and three were fired at increasing temperatures (600 C°, 900 C°, 1200 C°) in order to simulate different ancient production technologies, from low temperatures-fired pottery to the finest porcelain. The firing procedure, carried out in a static atmosphere in a L5/12/B170 Nabertherm GmbH (Lilienthal/Bremen, Germany) oven, consisted in a heating step from 25°C to the maximum temperature at 120°C/h, a isothermal phase for 10 minutes and an overnight cooling. Moreover, a second series of the SRM 98b standard was also prepared by moistening and kneading the clay powder, with the aim to better simulate true artefacts production. For these samples the firing step was conducted at 400 C° (in order to completely dehydrate the sample), 600 C°, 900 C° and 1200 C°, respectively. The described procedures and the resulting samples are summarized in Table 1.

Sample name	Raw material	Preparation procedure	Firing temperature
CL1	SRM 98b (Clay)	Hydraulic press	-
CL2	SRM 98b (Clay)	Hydraulic press	600 C°
CL3	SRM 98b (Clay)	Hydraulic press	900 C°
CL4	SRM 98b (Clay)	Hydraulic press	1200 C°
CL1k	SRM 98b (Clay)	Kneading moistened clay	400 C°
CL2k	SRM 98b (Clay)	Kneading moistened clay	600 C°
CL3k	SRM 98b (Clay)	Kneading moistened clay	900 C°
CL4k	SRM 98b (Clay)	Kneading moistened clay	1200 C°
CE1	SARM 69 (Ceramic)	Hydraulic press	-
CE2	SARM 69 (Ceramic)	Hydraulic press	600 C°
CE3	SARM 69 (Ceramic)	Hydraulic press	900 C°
CE4	SARM 69 (Ceramic)	Hydraulic press	1200 C°

Table 1: List of the samples with the corresponding preparation procedures.

The certified compositions of SRM 98b clay and SARM 69 ceramic are reported in Table 2

	Li	Na	Mg	Al	Si	K	Ca	Sc	Ti	Cr	Mn	Fe	Co	Ni	Cu	Zn	Rb	Sr	Zr	Ba	LOI*	Tot
		Na_2O	MgO	Al_2O_3	SiO_2	K_2O	CaO	Sc_2O_3	TiO_2	Cr_2O_3	MnO	FeO	CoO	NiO	CuO	ZnO	Rb_2O	SrO	ZrO_2	BaO		
SRM 98b																						
Elemental wt%	**0.022**	**0.150**	**0.36**	**14.3**	**26.7**	**2.81**	**0.076**		**0.81**	**0.0119**	**0.0116**	**1.18**	*0.0016*			*0.011*	*0.018*	**0.0189**	*0.022*		7.5	46.43
Oxides wt%		0.202	0.59	27.0	57.0	3.38	0.106		1.35	0.0174	0.0150	1.52	*0.0020*			*0.014*	*0.020*	0.0223	*0.030*			91.27
Normalized oxides wt%		0.221	0.65	29.6	62.4	3.71	0.116		1.48	0.0190	0.0164	1.66	*0.0022*			*0.015*	*0.022*	0.0245	*0.033*			100.00
SARM 69																						
Elemental wt%			1.12	7.62	31.20	1.63	1.69	0.0020	0.47	**0.0223**	0.10	5.02	**0.0028**	**0.0053**	**0.0046**	**0.0068**	*0.0066*	*0.0109*	*0.0271*	**0.0518**	*3.6*	49.03
Oxides wt%		*0.79*	**1.85**	**14.4**	**66.6**	**1.96**	**2.37**	**0.0031**	**0.777**	0.0652	**0.129**	**6.46**	0.0036	0.0067	0.0058	0.0085	*0.0072*	*0.0129*	*0.0366*	0.0578		95.54
Normalized oxides wt%		*0.83*	1.94	15.1	69.7	2.05	2.48	0.0032	0.813	0.0682	0.135	6.76	0.0037	0.0071	0.0060	0.0089	*0.0076*	*0.0135*	*0.0383*	0.0605		100.00

Table 2: Certified composition of SRM 98b clay and SARM 69 ceramic. Significant digits are equal to certified digits. In italic are reported tentative, not certified values. In bold are reported values listed on the certificates of analysis, the other values are calculated. *LOI=Loss on Ignition (determined at 1100°C for standard SRM 98b and at a not specified temperature for standard SARM 69).

2.2 Scanning Electron Microscopy coupled with Energy Dispersive X-ray Spectrometry (SEM-EDS)

In order to validate the results, analyses were performed by using two Scanning Electron Microscopes, an EVO-50 Zeiss and a Cambridge S-360 SEM equipped with an Oxford Instruments INCA Energy 200 EDS spectrometer and a X-Act3 SDD-EDS detector, respectively. All measurement were performed on polished section obtained by cutting the samples, encompassing them in an acrylic resin and subjecting the impregnated sections to an abrasive treatment on silicon carbide papers with a 500 and 1000 grit size and subsequently to a polishing step with a 1 μm diamond paste on special clothes. The polished sections were then mounted on aluminium stubs using carbon tape and they were covered with a coating of graphite using a coating unit SCD 050 Sputter Coater (Bal-Tec, Scotia, NY, USA). The SEM-EDS calibration was performed using the polished and carbon-coated 53 Minerals Standard (Structure Probe, Inc., West Chester, PA) and quantitation was performed using Oxford Instruments XPP correction. Two different configurations were used, setting the electron beam at 20 and 15 keV, respectively, for the INCA Energy 200 EDS spectrometer and for the X-Act3 SDD-EDS detector, in order to test any compositional difference depending on the different volumes involved in the generation of the analytical signals. The

analyses were performed at 200X magnification to obtain adequately representative data. This corresponds, on our instruments, to rectangles of approximately 1 mm^2. The analyses were performed, in both configurations, by scanning four areas for each sample. Each EDS spectrum (1024 channels, 10 eV/ch), contains about $4x10^5$ counts. Due to the Limit of Detection of the EDS spectrometers using an electron beam, universally homologated in the 0.1-0.3 wt% range (depending on the element of interest) (Newbury and Ritchie, 2013), the quantification was limited to 8 elements, namely Na, Mg, Al, Si, K, Ca, Ti and Fe.

2.3 Micro-X Ray Fluorescence (µXRF) Spectrometry

An Eagle III XPL Micro-Xray Fluorescence Spectrometer equipped with Rh X-ray tube, poly-capillary (spot size =30µm) and six primary filters was used, all measurements were performed in vacuum. The Fundamental Parameters with Standards (FP-STD) method and Lucas-Tooth & Pine (LTP) correction (Lucas-Tooth and Pyne, 1963) implemented in EDAX Vision32 software were both applied for quantitation. The glass standards used for major elements calibration are both natural and synthetic glass. The natural glass standards are (i) ALV 981, a tholeiite glass from East Pacific Rise; (ii) CFA 47, a trachyte obsidian from the Phlegrean Fields (Italy); and (iii) OSS, a liparite obsidian from Lipari (Italy) (Metrich and Clocchiatti, 1989; Vaggelli et al., 1999).

The synthetic glass standards are (i) SRM 620, produced and certified by the American National Institute of Standard and Technology (NIST); and (ii) SGT 7 and SGT 10, produced and certified by the Society of Glass Technology (SGT). A Rh X-ray tube excitation at 30kV and 300µA with no primary filter was used to measure the same elements selected for the SEM-EDS analyses. This configuration, although with limited sensitivity, allows to analyze all the elements with energy above 1 keV (z> = 11). To improve the reproducibility of the analyses the largest available spot size (165 µm diameter) was used. The sum spectra of 12 of these measures on adjacent areas produce the detected composition on a total area of approximately 0.3 mm^2. This procedure was repeated

four times in different zones of the sample. Mean and standard deviation values reported in the results section arise from these repetitions.

2.4 Thermo-Gravimetric Analysis (TGA)

Thermo-Gravimetric Analysis (TGA) was conducted by a SDTQ600 Thermal Analyzer (TA Instruments, New Castle, DE, USA) using a standard of aluminium oxide. The appropriate amount (around 10 mg) of each sample was heated from 35 to 1200 °C with a temperature gradient of 10 °C/min under an air flow of 100 ml/min.

2.5 Semi-quantitative method for porosity determination

Considering the initial grain size of the clay standard (<10 μm), BSE images at a high magnification (≥ 1000X) were chosen for the semi-quantitative evaluation of the porosity. High probe current and contrast were used in order to separate very low atomic number components (i.e. sodium) from those belonging to voids on surface. The determined threshold of grey was utilized to obtain a binary image (Figure 1), the calculation was carried out by simply dividing the number of black pixels of this image by the total number of pixels ($\approx 10^6$ pixels) by means of the INCA microprobe software. A similar procedure was already adopted in order to evaluate the close porosity in porcelain (Correia et al., 2007). If this calculation is made on different areas (4 in the present case) on different planes within the sample, it is possible to approximately evaluate (standard deviation) the reliability of this estimate in terms of volume.

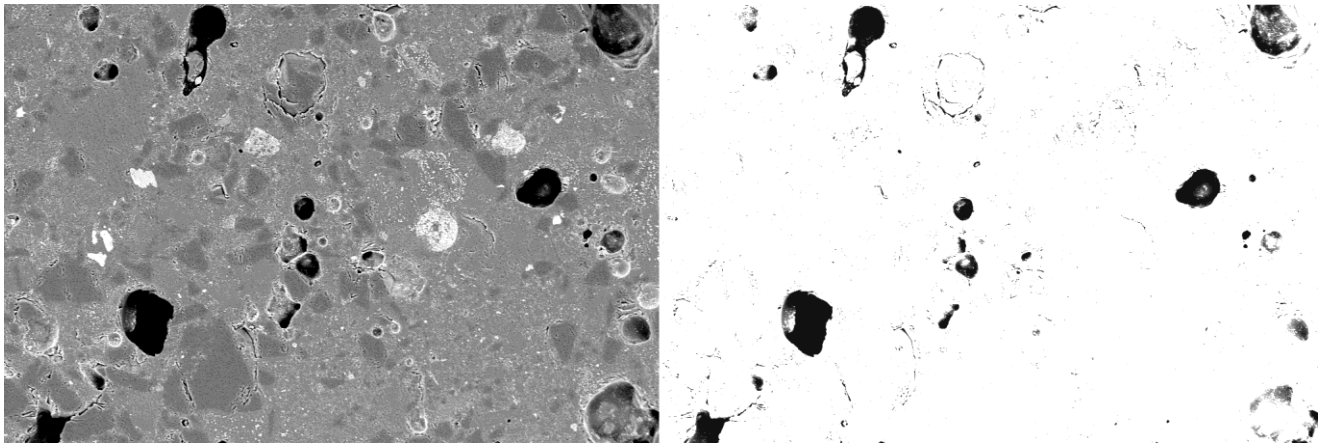

Figure 1: CE4 sample BSE image, 1000X magnification (left) and the corresponding binary images (right) obtained by the grey threshold application.

3. RESULTS AND DISCUSSION

3.1 SEM-EDS

Tables 3a and 3b illustrate the mean values and the corresponding standard deviations of the SEM-EDS analyses carried out in the two configurations (at 15 and 20 keV), respectively. All the values satisfy the 3-σ criterion for a specific element in each analysis. The results are expressed as oxide weight % and then normalized to 100, the oxygen has been calculated by stoichiometry.

	E_0=15keV								E_0=20keV							
Sample	**Na_2O**	**MgO**	**Al_2O_3**	**SiO_2**	**K_2O**	**CaO**	**TiO_2**	**FeO**	**Na_2O**	**MgO**	**Al_2O_3**	**SiO_2**	**K_2O**	**CaO**	**TiO_2**	**FeO**
CL1	0.27	0.94	31.22	58.71	4.67	0.46	1.65	2.08	0.30	0.78	30.73	59.28	4.29	1.01	1.60	2.01
CL2	0.31	0.81	30.51	59.07	4.76	0.73	1.63	2.18	0.35	0.75	30.54	59.79	4.24	0.81	1.56	1.95
CL3	0.24	0.83	30.81	59.24	4.64	0.14	1.71	2.39	0.26	0.71	30.95	60.72	3.96	0.19	1.37	1.84
CL4	0.25	0.67	28.70	62.65	4.07	0.16	1.54	1.96	0.24	0.58	29.21	62.78	3.77	0.14	1.50	1.78
CL1k	0.27	0.76	31.67	58.70	4.72	0.24	1.61	2.03	0.25	0.77	30.80	59.80	4.47	0.18	1.71	2.02
CL2k	0.49	0.83	29.75	57.30	5.00	2.74	1.63	2.25	0.56	0.96	29.64	58.73	4.47	1.91	1.70	2.03
CL3k	0.51	1.11	29.82	58.28	4.73	1.69	1.63	2.23	0.53	1.09	29.99	59.03	4.50	0.95	1.75	2.16
CL4k	0.26	0.70	28.54	62.89	4.02	0.19	1.58	1.81	0.27	0.75	28.91	62.68	3.81	0.16	1.58	1.84
CE1	0.72	1.86	17.38	62.65	2.91	2.73	0.92	10.83	0.81	1.93	17.65	64.29	2.55	2.80	0.94	9.04
CE2	0.73	1.89	16.62	63.50	2.85	2.93	0.94	10.54	0.84	1.76	16.84	65.35	2.43	2.64	0.82	9.31
CE3	0.77	2.03	16.72	63.37	2.66	2.88	0.92	10.65	0.91	1.83	16.72	63.57	2.52	3.10	0.89	10.46
CE4	0.92	1.86	14.73	69.26	2.26	2.57	0.91	7.47	0.93	1.75	14.85	69.73	2.16	2.60	0.66	7.31

Table 3a: SEM-EDS normalized mean values (at 15 and 20 keV, respectively), expressed as oxide wt%.

	E_0=15keV								E_0=20keV							
Sample	**Na_2O**	**MgO**	**Al_2O_3**	**SiO_2**	**K_2O**	**CaO**	**TiO_2**	**FeO**	**Na_2O**	**MgO**	**Al_2O_3**	**SiO_2**	**K_2O**	**CaO**	**TiO_2**	**FeO**
CL1	0.04	0.13	0.49	0.50	0.15	0.12	0.11	0.16	0.09	0.10	0.33	0.23	0.10	0.10	0.09	0.03
CL2	0.06	0.02	0.44	0.52	0.11	0.15	0.08	0.14	0.05	0.07	0.10	0.27	0.05	0.31	0.08	0.13
CL3	0.01	0.02	0.15	0.71	0.07	0.10	0.07	0.83	0.10	0.05	0.25	0.49	0.07	0.03	0.06	0.06
CL4	0.01	0.02	0.29	0.43	0.03	0.03	0.05	0.14	0.06	0.04	0.31	0.24	0.09	0.01	0.08	0.15
CL1k	0.08	0.05	0.39	0.36	0.06	0.05	0.09	0.13	0.06	0.08	0.18	0.37	0.1	0.03	0.09	0.19
CL2k	0.12	0.06	0.31	0.60	0.10	0.66	0.05	0.16	0.04	0.05	0.02	0.25	0.07	0.15	0.06	0.04
CL3k	0.10	0.04	0.26	0.37	0.11	0.52	0.08	0.13	0.06	0.19	0.20	0.1	0.12	0.14	0.07	0.15
CL4k	0.04	0.02	0.42	0.52	0.10	0.04	0.10	0.12	0.07	0.07	0.21	0.26	0.14	0.03	0.07	0.06
CE1	0.02	0.07	0.34	0.83	0.10	0.14	0.06	0.21	0.13	0.07	0.53	0.45	0.06	0.07	0.04	0.37
CE2	0.08	0.14	0.28	0.93	0.08	0.35	0.08	0.42	0.04	0.09	0.33	0.22	0.04	0.09	0.06	0.15
CE3	0.03	0.06	0.17	0.40	0.04	0.11	0.11	0.24	0.11	0.04	0.15	0.52	0.02	0.17	0.10	0.19
CE4	0.06	0.06	0.06	0.42	0.03	0.17	0.11	0.43	0.11	0.02	0.13	0.33	0.08	0.12	0.07	0.11

Table 3b: SEM-EDS normalized standard deviation values (at 15 and 20 keV, respectively), expressed as oxide wt%.

Table 3a: SEM-EDS normalized mean values (at 15 and 20 keV, respectively), expressed as oxide wt%. Table 3b: SEM-EDS normalized standard deviation values (at 15 and 20 keV, respectively), expressed as oxide wt%.

Table 3a highlights an apparent composition change vs temperature: for example, SiO_2 content shows a general relative upward trend at the temperature increase while K_2O and FeO typically show downward trends. All these variations appear most evident in the 900÷1200°C range and are quite comparable for the two instrumentations.

Sample	**15keV vs 20keV**	**15keV vs STD**	**20keV vs STD**
CL1	0.37	1.51	1.25
CL2	0.33	1.34	1.06
CL3	0.63	1.28	0.78
CL4	0.26	0.37	0.19
CL1k	0.52	1.57	1.06
CL2k	0.63	2.11	1.49
CL3k	0.41	1.65	1.30
CL4k	0.17	0.43	0.27
CE1	0.92	2.97	2.20
CE2	0.89	2.62	1.80
CE3	0.15	2.57	2.52
CE4	0.21	0.22	0.16

Table 4: RMS difference values (expressed as wt%) for each sample between the two configurations (15 and 20 keV) and for each configuration with respect to the certified values.

Table 4 illustrates the Root Mean Square (RMS) difference values (expressed as wt%) for each sample, between the two configurations (15 and 20 KeV) and for each configuration with respect to the certified values. The differences calculated between the two configurations are generally lower than those obtained for each configuration with respect to the certified values and the detected values for the SARM 69 ceramic standard showed generally higher differences from the certified data then the SRM 98b clay. In general, the smaller differences were observed at the highest temperature (1200°C; i.e. for the samples CL4, CL4k, CE4). Due to the very limited divergence between the two configurations (15 and 20 keV), the values obtained at 15 keV (SDD detector) were chosen for all the following evaluations.

To estimate the specific trend for each element, mean detected values were compared with the certified composition; the relative percent differences are tabulated in Table 5.

Sample	Na_2O	MgO	Al_2O_3	SiO_2	K_2O	CaO	TiO_2	FeO
CL1	22	45	5	-6	26	297	11	25
CL2	40	25	3	-5	28	529	10	31
CL3	9	28	4	-5	25	21	16	44
CL4	13	3	-3	0	9	38	4	18
CL1k	22	17	7	-6	27	107	9	22
CL2k	122	28	0	-8	35	2262	10	36
CL3k	131	71	1	-7	27	1357	10	34
CL4k	18	8	-4	1	8	64	7	9
CE1	-13	-5	14	-11	41	9	12	59
CE2	-12	-3	9	-9	38	17	14	55
CE3	-7	5	11	-9	30	16	13	58
CE4	11	-4	-3	-1	10	4	12	10

Table 5: Relative percent difference between obtained mean values (SEM-EDS, 15 keV) vs certified data (expressed as normalized oxides wt%).

The highest differences were observed for the CaO values in the case of CL samples, while relatively quite relevant variations were spotted for Na_2O, K_2O and FeO for both standards and for MgO for the clay standard. While the high values for Na_2O and MgO are quite understandable due to their low concentration values, K_2O and FeO data are more alarming, especially for CE samples, in which iron is a major element (certified FeO wt%= 6.46). It is essential to point out that standard

deviation data for measured FeO mean values are quite low (Table 3b) and that the RMS difference values between the two configurations (15 and 20 KeV) suggest a good reproducibility, indicating that the high percent difference for FeO should be a matter of accuracy. At last, difference values are basically lower for both standards at the highest temperature (1200°C, samples CL4, CL4k and CE4).

3.2 µXRF

The mean and standard deviation values (expressed as normalized oxide wt%) obtained from 4 different areas on each sample are reported in Table 6a and Table 6b, respectively.

Sample	Na_2O	MgO	Al_2O_3	SiO_2	K_2O	CaO	TiO_2	FeO
CL1	0.13	0.78	24.65	66.46	4.08	0.78	1.38	1.75
CL2	0.21	0.63	27.71	62.42	4.97	0.56	1.63	1.86
CL3	0.20	0.59	28.30	62.30	4.93	0.40	1.72	1.56
CL4	0.14	0.44	28.96	61.98	4.67	0.40	1.66	1.75
CL1k	0.11	0.57	28.18	62.03	5.14	0.39	1.66	1.91
CL2k	0.16	0.55	27.30	62.22	5.33	0.68	1.79	1.96
CL3k	0.17	0.76	28.28	61.57	5.04	0.52	1.75	1.92
CL4k	0.20	0.54	27.06	63.32	4.90	0.37	1.73	1.87
CE1	0.63	1.91	17.24	68.82	2.98	1.92	0.76	5.74
CE2	0.65	1.75	17.59	67.29	2.72	2.07	0.85	7.07
CE3	0.62	1.97	16.41	68.56	2.54	2.17	0.62	7.11
CE4	0.70	2.15	18.04	66.42	2.81	2.15	0.77	6.95

Table 6a: µXRF mean values for major and minor elements expressed as normalized oxides wt% (FP-STD calculation).

Sample	Na_2O	MgO	Al_2O_3	SiO_2	K_2O	CaO	TiO_2	FeO
CL1	0.04	0.13	0.73	1.06	0.21	0.01	0.09	0.12
CL2	0.09	0.05	0.75	2.33	0.08	0.04	0.18	0.07
CL3	0.05	0.09	0.74	2.44	0.22	0.04	0.19	0.17
CL4	0.03	0.04	0.56	1.37	0.2	0.02	0.19	0.18
CL1k	0.03	0.11	0.42	2.48	0.19	0.06	0.32	0.19
CL2k	0.04	0.08	1.2	0.92	0.16	0.03	0.08	0.07
CL3k	0.09	0.13	0.51	1.21	0.2	0.08	0.28	0.08
CL4k	0.07	0.08	1.70	2.10	0.27	0.03	0.14	0.22
CE1	0.09	0.19	0.66	1.61	0.24	0.02	0.22	0.21
CE2	0.11	0.33	0.49	2.92	0.22	0.07	0.38	0.22
CE3	0.13	0.26	1.41	1.08	0.19	0.04	0.09	0.08
CE4	0.12	0.32	0.60	1.42	0.24	0.09	0.33	0.09

Table 6b: µXRF standard deviation values for major and minor elements expressed as normalized oxides wt% (FP-STD calculation).

Table 7 illustrates the relative percent differences between the μXRF mean values (Table 6a) and the certified concentrations. Also in the case of μXRF analysis, CaO shows the greatest changes (for the two CL series of samples) and relatively high variations are observed for Na_2O and in lower measure for MgO. As for SEM-EDS, the relatively high values for Na_2O and MgO are not so alarming due to their low concentration values. Less understandable are the quite substantial differences for K_2O while FeO variations are more limited than in the case of SEM-EDS.

Sample	Na_2O	MgO	Al_2O_3	SiO_2	K_2O	CaO	TiO_2	FeO
CL1	-41	20	-17	7	10	572	-7	5
CL2	-5	-3	-6	0	34	383	10	12
CL3	-10	-9	-4	0	33	245	16	-6
CL4	-37	-32	-2	-1	26	245	11	5
CL1k	-50	-12	-5	-1	38	236	12	15
CL2k	-28	-15	-8	0	43	486	21	18
CL3k	-23	17	-4	-1	36	348	18	16
CL4k	-10	-17	-9	1	32	219	17	13
CE1	-24	-2	14	-2	45	-23	-7	-15
CE2	-22	-10	16	-4	32	-17	5	4
CE3	-25	1	8	-2	23	-13	-24	5
CE4	-16	11	19	-5	37	-13	-5	3

Table 7: Relative percent difference between μXRF (FP-STD) mean values and the certified composition (expressed as normalized oxides wt%).

As a general rule, a tendency towards a SiO_2 underestimation and a CaO, K_2O, TiO_2 and FeO overestimation (few exceptions to this trend are observed for the μXRF data on the CE series) was noticed for both techniques. Moreover, for most elements the deviations are generally lower at higher temperatures.

3.3 TGA

The obtained analytical totals for the SEM-EDS and μXRF data on the CL and CE series were systematically lower than 100, as expected, and they were normalized to 100%, as usual. The difference to 100% is partially explicable accounting for compounds present in ceramic materials

but not quantifiable neither by SEM-EDS nor by XRF (i.e. H_2O and CO_2), constituting the so-called Loss On Ignition (LOI). Thermo-gravimetric analyses were performed to evaluate the LOI at the different temperatures. The percent total losses in weight (wt%) as a function of temperature for standards SRM 98b (clay) and SARM 69 (ceramic) are reported in Table 8. Standard SRM 98b (clay) loses around 7 wt% until 600°C due to adsorbed and chemically bound water and an additional 1.5% until 900°C corresponding to CO_2 removal due to the decomposition of carbonates (Moropoulou et al., 1995). Standard SARM 69 (ceramic) loses around 3.5 wt% up to 600°C and an additional 0.5% between 600°C and 900°C. Thereafter the weight of both standards remains practically stable up to 1200°C.

Standard	600°C	900°C	1200°C
SRM 98b (Clay)	-6.62	-8.17	-8.31
SARM 69 (Ceramic)	-3.43	-3.86	-4.08

Table 8: Standards SRM 98b (clay) and SARM 69 (ceramic) cumulative losses (wt%) obtained by TGA as a function of temperature.

3.4 Porosity

As known from the scientific literature (Freestone, 1982; Ting et al., 2015) low analytical totals are also ascribable to a high porosity and this is fundamentally the reason for the adoption of the procedure of normalization for compositional data. To evaluate the influence of the degree of porosity on the analytical total and in order to compare results obtained on samples prepared with different procedures, and finally with the respective certified values, at least a semi-quantitative estimate of the voids within the samples was required.

Due to the fact that in the case of pottery and porcelain most of the porosity is ascribable to close pores, the typical techniques based on liquids or gases sorption are not suitable for these materials, the porosity semiquantitative evaluation was performed as described in the Materials and Methods subsection. Figure 2 illustrates the mean and standard deviation values (obtained

from the 4 measured areas) of the porosity for the three series of samples. The results show a general increasing trend up to 900 ° C for all CL, CLk and CE series (except for sample CL2k) and then an abrupt decrease at higher temperatures. The highest value (36 area %) is observed for sample CL3 (at 900°C) and the lowest (5 area %) for sample CE4 (at 1200°C). As for standard deviations, the values are typically very limited (lower than 5%), with the exception of samples CE1 and CE2, strongly suggesting that the measure of 4 areas on different planes can reasonably represent the sample volume.

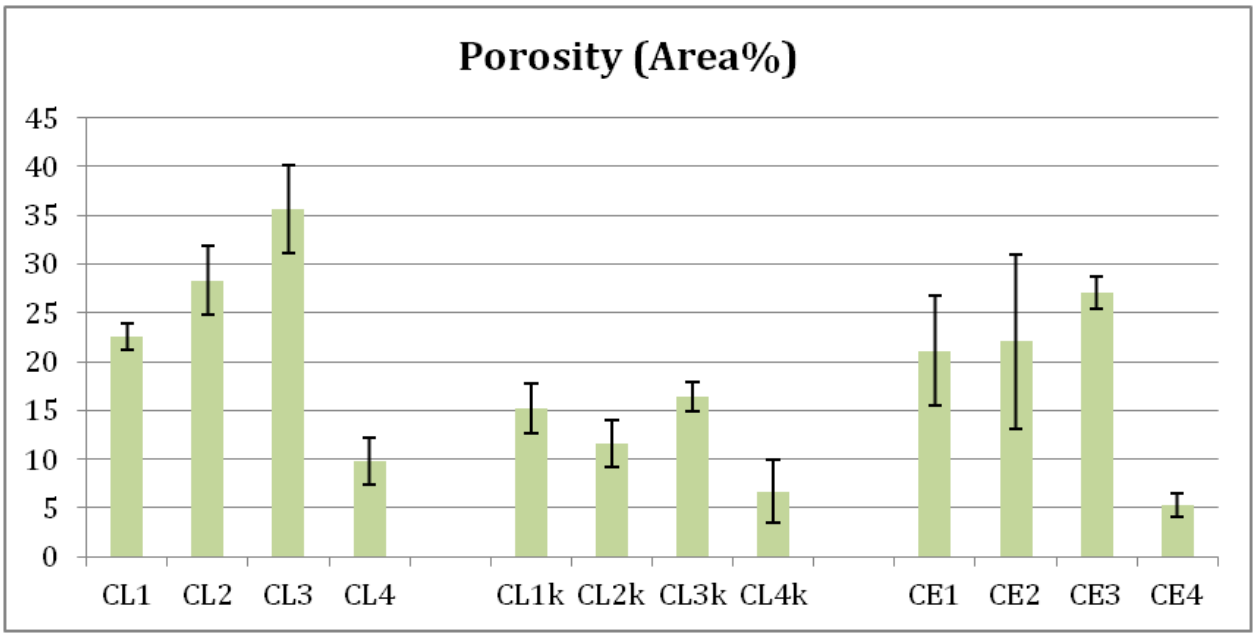

Figure 2: Estimated mean porosity values (area %) with the corresponding standard deviations.

The porosity was also estimated on historical (a fragment of porcelain, Figure 3, left) and on archaeological (a ceramic sherd, Figure 3, right) objects and the obtained results were 4.7% and 18.4% respectively, demonstrating that the obtained standards are representative for real materials, as far as the porosity is concerned.

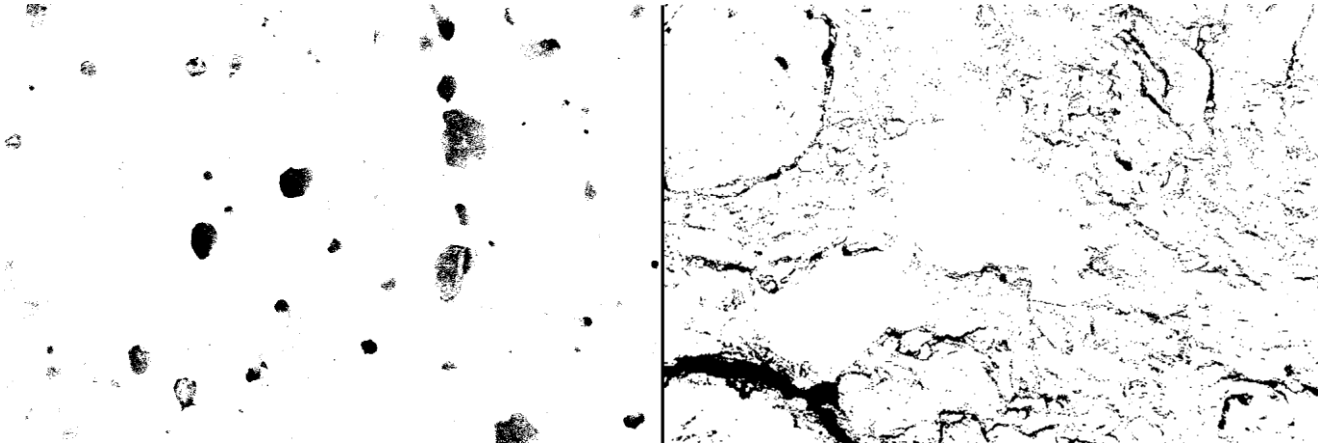

Figure 3: Binary SEM-BSE images (1000X) of a XVIII century Piedmontese porcelain fragment (left) and of a Bronze Age ceramic sherd (right) (estimated firing temperature 850-950°C (Davit et al., 2014)).

3.5 Analytical total vs porosity

The examination of the trends emerging from Figure 2 underlines the great variability of the relative porosity vs temperature. The highlight tendency is totally consistent with the presence of a high amount of intra-grain voids in the raw materials and after firing at low temperatures, while at increasing temperatures phase transformations and carbonates decomposition occur until the beginning of vitrification and voids contraction, finally leading to the formation of more regular pores. The temperature at which these transformations take place depends on the chemical and mineralogical composition and on the conditions (atmosphere) of the firing step, as diffusely reported in the scientific literature, for example by Correia et al. (2007) and Maniatis and Tite (1981).

As for SEM-EDS results Freestone even pointed out that the obtained analytical total could be used as an estimate of porosity (Freestone, 1982). The porosity (area, or volume%), the corresponding LOI (Δwt% up to 1200 °C, obtained by TGA analyses) and the analytical total (oxides wt%) values resulting from the not normalized results were compared together for each sample. In order to obtain the not normalized compositional data, the mean analytical total between the µXRF (LTP calculation) and SEM-EDS (in the two analytical conditions) results was calculated, with

the corresponding standard deviations. The obtained values are reported in Figure 4 (left). The relatively low standard deviation data (lower than 10% for all the samples, except for CL3) indicate a good concordance between SEM-EDS and µXRF results. Comparing Figures 2 and 4 (left) it can be observed that mean analytical total values basically show an opposite trend with respect to the estimated porosity. This trend is directly showed by the bi-plot in figure 4 (right), showing the quasi-linear reverse correlation between mean analytical total and porosity. The points with the major deviation from the linear trend represent unfired (CE1 and CL1) and low temperature fired (CL1k) samples, i.e. samples with higher LOI. This result, despite the caution due to the semi-quantitative nature of the procedure for measuring porosity, confirms the plain correlation between analytical total and porosity.

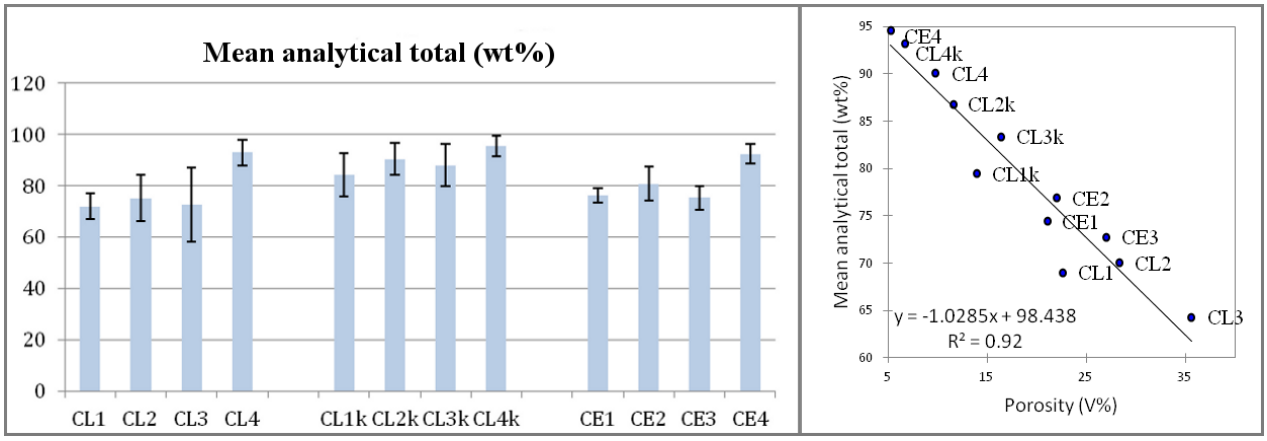

Figure 4: Mean analytical totals (oxides wt%) obtained by SEM-EDS and µXRF data with the corresponding standard deviations for each sample (left). Bi-plot of mean analytical total vs. porosity (right).

3.6 Accuracy vs relative standard-sample porosity

Knížek and Jurek (1994) also describe the influence of the porosity on the analyzed volume with consequent absorption variation versus the energy of the selected analytical line, for the electron microprobe techniques. Knížek and Jurek paper specifically illustrates that a variable proportionality coefficient, inversely proportional to the specific line energy, is needed for the normalization in the case of porous materials, if the mass range of the constituting elements is

wide. In the case of ceramic and porcelain objects the major and minor elements usually range from Na to Fe, with analytical K-line from 1 to 6.4 keV, and this would account for the higher errors observed in our data for the "heavier" elements such as K and Fe, which are overestimated. The selective absorption of the X-ray emitted by "lighter" elements is balanced by the normalization, while for the "heavier" elements the absorption is negligible and the normalization leads to overestimate the concentration. This difference is illustrated in Figure 5 (SEM-EDS), where is evident that normalized values are much more accurate for the "lighter" elements, while "heavier" elements are overestimated and not normalized data fit better in this last case.

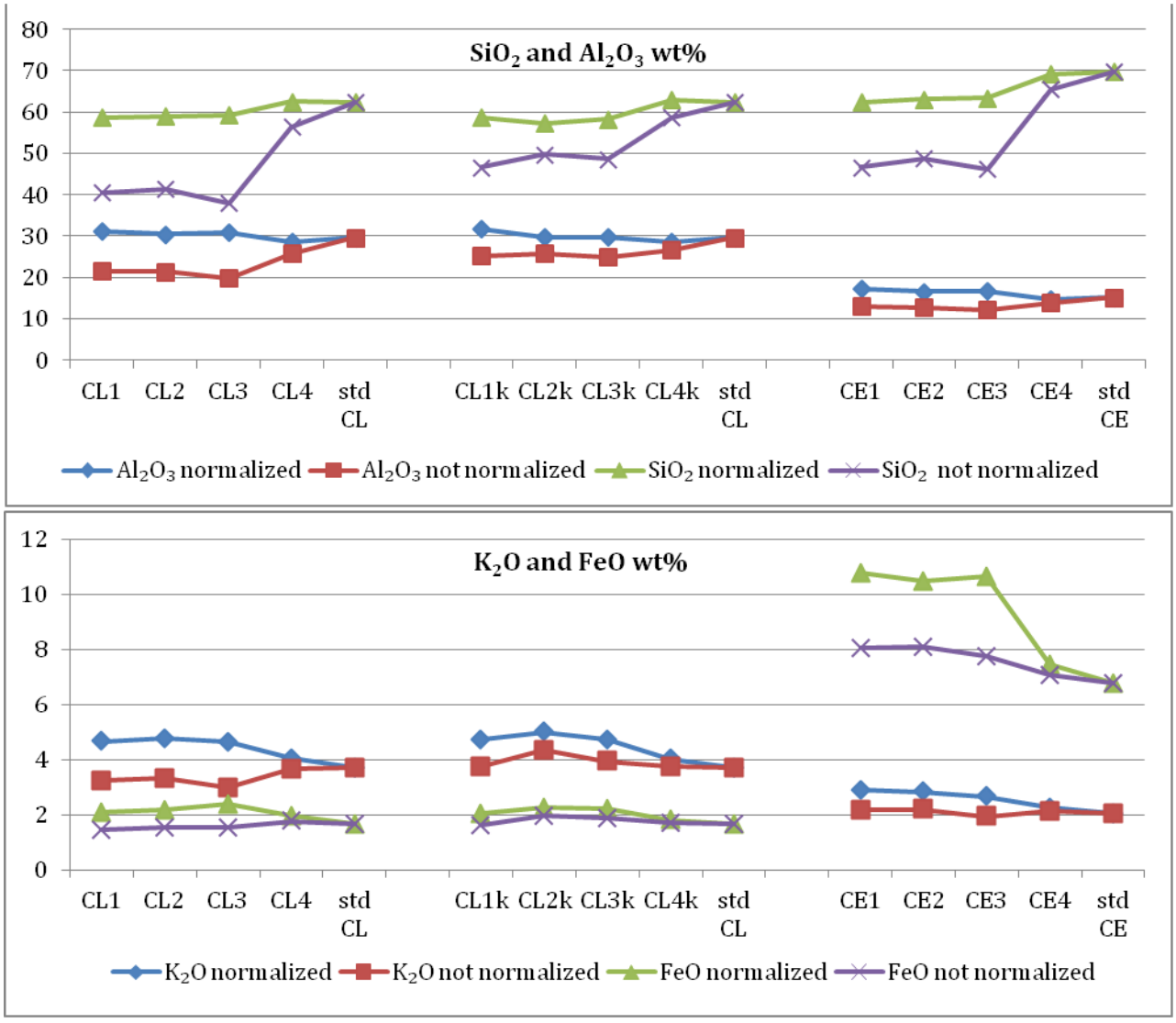

Figure 5: Comparison of the SEM-EDS normalized and not normalized values for SiO_2 and Al_2O_3 wt% (top) and for K_2O and FeO wt% (bottom).

Figure 6 shows similar trends for µXRF, as expected due to the same physical principle the detection in both techniques is based on.

Errors are due to the different path in the sample with respect to a non-porous material.

Moreover, being equal the signal source region, the medium density of the material is lower than expected, causing noticeable errors when the correction algorithm is applied. Therefore, even considering the great difference in the pathlength of the incident rays, this is a bulk effect for both techniques.

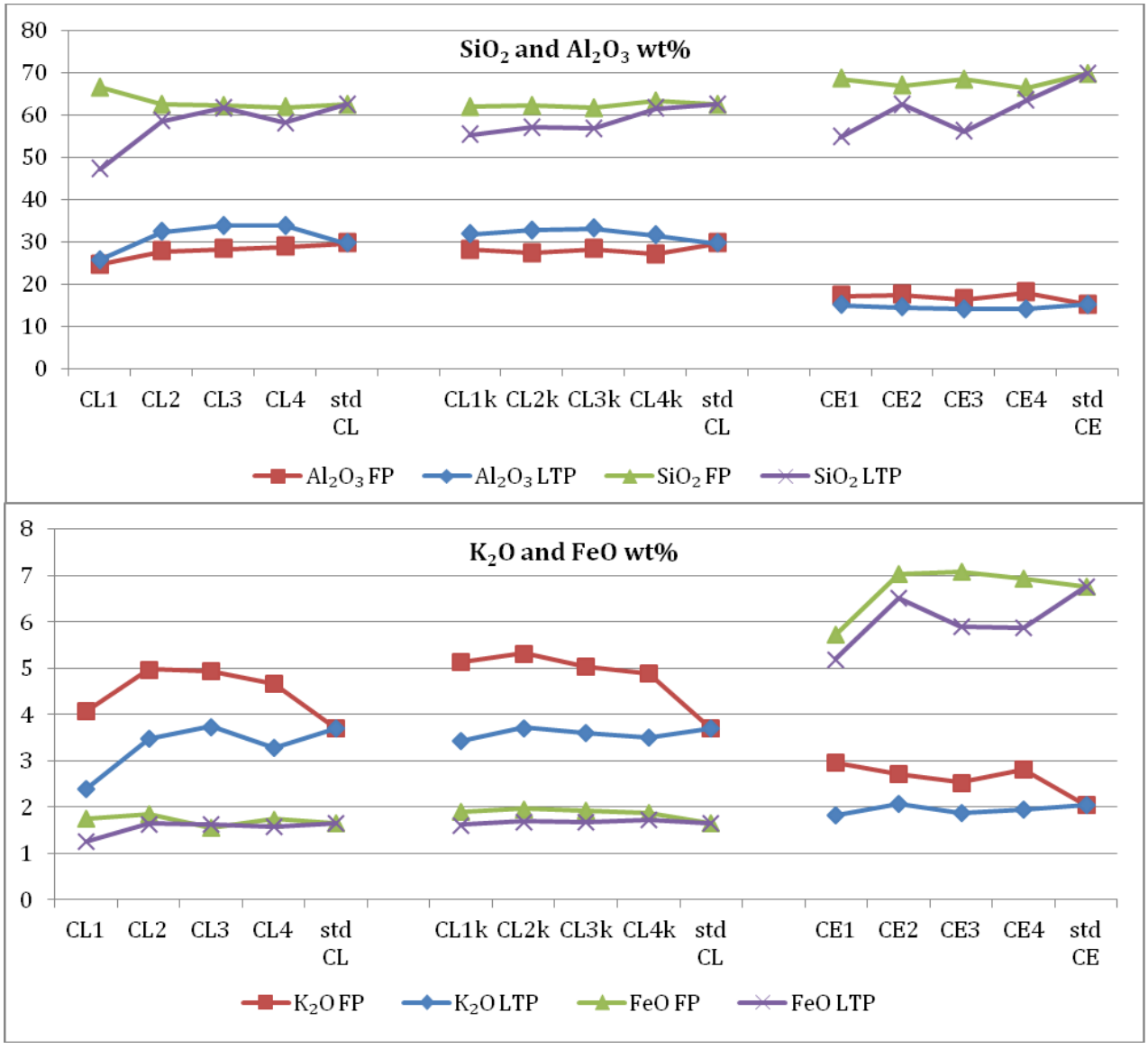

Figure 6: Comparison of the µXRF normalized (FP-STD) and not normalized (LTP) values for SiO_2 and Al_2O_3 wt% (top) and for K_2O and FeO wt% (bottom).

The possible solution to obtain corrected data for both “light” and “heavy” elements is to calculate the specific coefficients as suggested by Knížek and Jurek (1994), but this procedure is quite complex and not applicable to μXRF due to its resolution (minimum spot of tenth of μm). A more easily applicable alternative is to calibrate the instrument by using a standard with porosity as similar as possible to the sample under examination. Figure 7 illustrates CL1, CL2 and CL3 SEM-EDS oxide wt% values obtained by using samples CE1, CE2, CE3 and CL1k as calibration standards, compared to the values obtained using massive mineral standards calibration and to the certified data. The most accurate values are obtained with samples CE3 and CL1k as calibration standards. This outcome is expected for CL1k due to the identical composition of the analyzed samples and of the calibration standard. In the case of sample CE3 the result is much more intriguing due to the similarity of CE3 porosity to the porosity of the series CL1-CL2-CL3 (Figure 2). This observation indicates that with a standard of porosity comparable to an eventual archeological and/or historical ceramic object the SEM-EDS results are highly accurate even for a standard of different composition (as inevitable in the case of real samples). The Figure also shows that the massive minerals and the not fired sample CE1 were the worst calibration standards in all the examined cases.

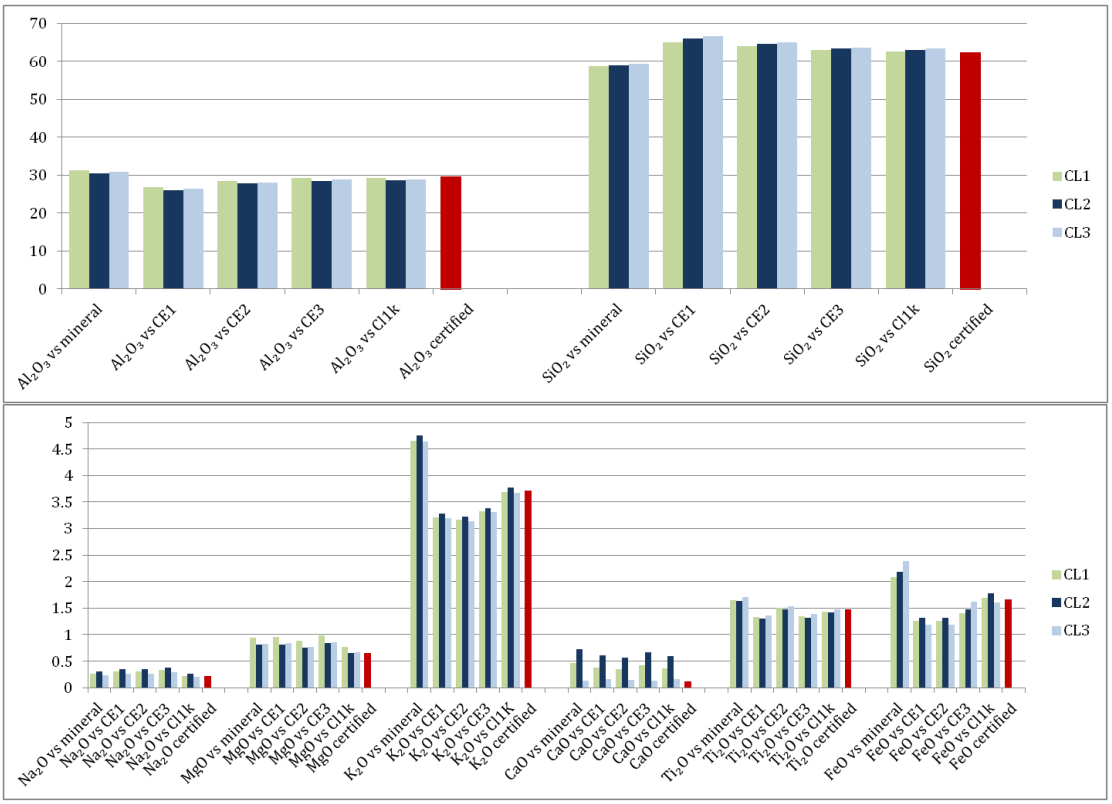

Figure 7: Al_2O_3 and SiO_2 (top) and Na_2O, MgO, K_2O, CaO, TiO_2 and FeO (bottom) normalized oxides wt% for CL1, CL2 e CL3 samples analyzed by SEM-EDS calibrated versus massive mineral standards, CE1, CE2, CE3 and CL1k, and certified values.

As for the standards obtained at the highest temperature (1200°C), which should better simulate the case of porcelain, only a small improvement with respect to the massive minerals calibration was observed in samples CL4 and CL4k analyses when standard CE4 was used to calibrate (Figure 8). This is reasonably due to the high-fired standard low porosity, which makes the eventual error using massive mineral standards for calibration quite limited. On the other hand, standard CE1 (raw) has a too much different porosity and gives the worst results.

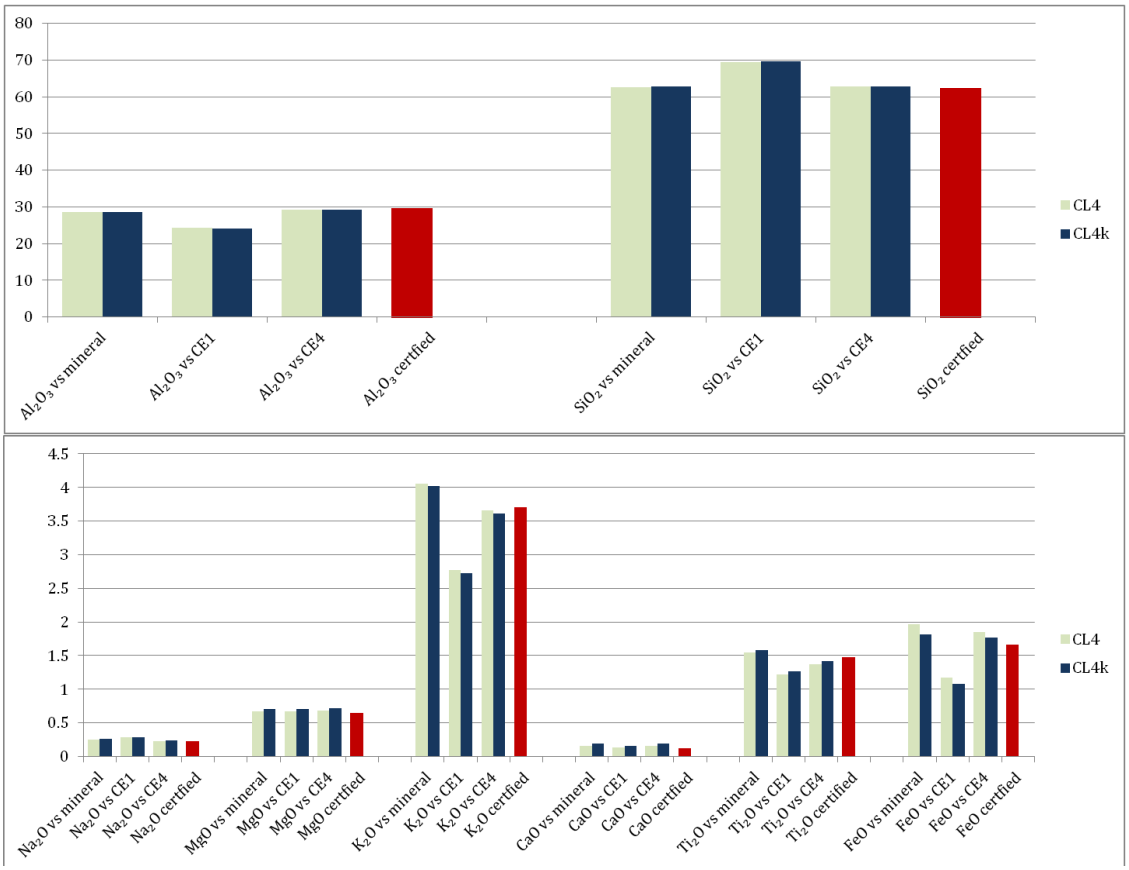

Figure 8: Al_2O_3 and SiO_2 (top) and Na_2O, MgO, K_2O, CaO, TiO_2, FeO (bottom) normalized oxides wt% for CL4 and CL4k samples analyzed by SEM-EDS calibrated versus massive mineral standards, CE1 and CE4, and certified values.

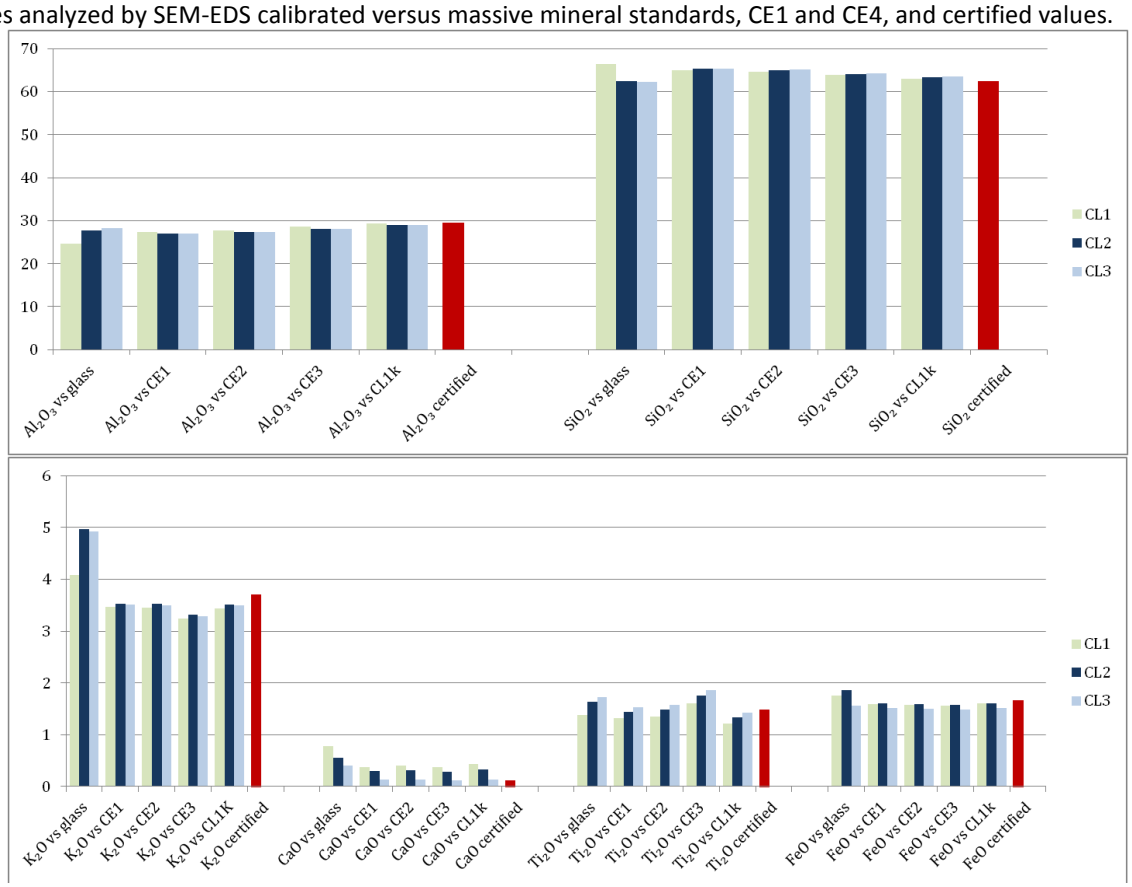

Figure 9: Al_2O_3 and SiO_2 (top) and K_2O, CaO, TiO_2, FeO (bottom) detected wt% for CL1,CL2 and CL3 samples when calibrated versus glass standards, CE1, CE2, CE3 and CL1k samples (µXRF, FP-STD calculation) and certified values.

In the case of µXRF (Figure 9) the tendencies are more complicated. Also in this case CL1k gives the best results, as expected, and an overall improvement is observed for the series CE1-CE2-CE3, that is the more the porosity of the standard becomes similar to the porosity of the samples, even if with some trend inversions. As far as the glass standards calibration is concerned, the results are not directly comparable due to the use of a combination of six standards instead of a single standard. However it is evident that the use of the series CE1-CE2-CE3 as standards shows better congruity for Al_2O_3, K_2O, CaO, TiO_2 and FeO while SiO_2 values are almost equivalent or even worse with respect to the glass standards calibration. Considering the low sensitivity of the technique towards Na and Mg, the variations of these elements were not plotted. As a general conclusion, also in the case of µXRF an overall (even if slighter than in the case of SEM-EDS) improvement is observed using a specifically prepared standard (CE3) instead of the typical glass standards.

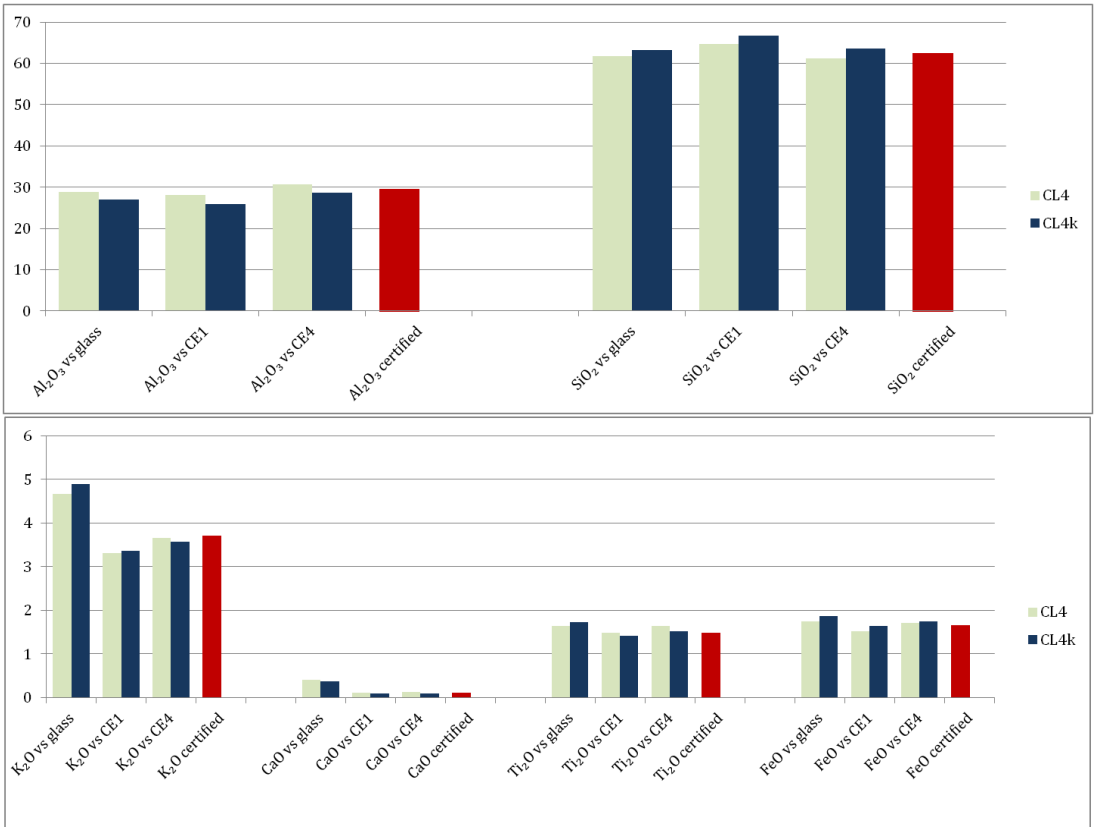

Figure 10: Al_2O_3 and SiO_2 (top) and K_2O, CaO, TiO_2, FeO (10b, bottom) detected wt% for CL4 and CL4k samples when calibrated vs glass standards, CE1, and CE4 samples (µXRF, FP-STD calculation) and certified values.

Eventually, calibrating CL4 and CL4k versus a high temperature fired standard (CE4, 1200°C) the results do not show a substantial difference with respect to the use of the glass standards in the case of Al_2O_3 and SiO_2, while the improvement is definite for K_2O and CaO and not negligible for FeO and TiO_2 (Figure 10). Also in this case the worst situation is showed for sample CE1 (raw).

As a general consideration, the results obtained for CaO both with SEM-EDS and μXRF are extremely fluctuating and scarcely accurate. This feature could be reasonably explained in terms of precision in the case of the SRM 98b standard (CaO = 0.106 wt%), but it is less explicable for standard SARM 69 showing a definitely higher CaO content (2.37 wt%), requiring a more in-depth analysis on materials containing different Ca contents.

The data showed in Figures 7, 8, 9 and 10 are summarized in Table 9 that reports the RMS differences between the certified compositions and the values obtained analyzing samples CL1, CL2, CL3, CL4 and CL4k with SEM-EDS and μXRF using massive mineral/glass standards and CE1, CE2, CE3, CL1k and CE4 as calibration standards. In the case of SEM-EDS there is an evident tendency of the RMS differences to decrease the more the estimated porosity of the sample and of the calibration standard are similar. On the other hand the situation is not so plain in the case of XRF, for which the trend observed for the series CE1-CE2-CE3 is comparable to SEM-EDS but the context is more complicated when the results obtained with the glass standards are taken into account.

	SEM-EDS							**μXRF**					
	mineral	**CE1**	**CE2**	**CE3**	**CL1k**	**CE4**		**glass**	**CE1**	**CE2**	**CE3**	**CL1k**	**CE4**
CL1	1.51	1.40	0.76	0.36	0.16		**CL1**	2.64	1.36	1.19	0.76	0.34	
CL2	1.34	1.80	1.05	0.60	0.44		**CL2**	0.95	1.59	1.40	0.97	0.51	
CL3	1.28	1.92	1.11	0.55	0.42		**CL3**	0.76	1.64	1.45	1.02	0.57	
CL4	0.37	3.16				0.20	**CL4**	0.57	1.13				0.67
CL4k	0.43	3.24				0.21	**CL4k**	1.22	2.34				0.59

Table 9: RMS differences between the certified compositions and the values obtained analyzing samples CL1, CL2, CL3, CL4 and CL4k with SEM-EDS (left) and μXRF (right) using massive minerals (for SEM-EDS)/glass (for μXRF) standards and CE1, CE2, CE3, CL1k and CE4 as calibration standards.

Finally, in order to examine the accuracy improvement for each element, Table 10 shows the accuracy for SEM-EDS results obtained on CL1, CL2 and CL3 samples using CE3 as calibration standard. Comparing these results with those reported in Table 5 a considerable improvement of accuracy for all elements (with the exception of Na and Mg), can be observed, especially for Si, K and Fe, in particular as regards CL3.

Sample	Na_2O	MgO	Al_2O_3	SiO_2	K_2O	CaO	TiO_2	FeO
CL1	49	51	-1	1	-1	262	-9	-15
CL2	72	29	-4	2	2	478	-11	-11
CL3	31	32	-3	2	-1	12	-6	-2

Table 10: Relative percent differences between obtained mean values using CE3 as calibration standards vs certified data (expressed as normalized oxides wt%), for SEM-EDS.

4. CONCLUSIONS

The present work evidenced that overestimated values are usually obtained for “heavy” elements in the compositional determination of ceramic and porcelain materials. This gap is particularly evident in the case of SEM-EDS data, but it is not negligible even for µXRF. The results clearly showed that the use of a standard characterized by a porosity similar to the porosity of the samples is advisable for the determination of chemical composition of ceramic materials, considerably increasing data accuracy. This observation is particularly essential in the temperature interval (600-900 °C) of the typical firing step of ancient pottery, which usually shows a porosity of even few tens percent in volume. All these considerations suggest that porosity determination is an important parameter to be considered for each newly examined ceramic class. In fact, the porosity data reported in the present work can not be considered all-purpose, since porosity is influenced not only by the firing temperature but also by the chemical composition and by firing conditions.

The proposed method for a semi-quantitative evaluation of ceramic and porcelain materials porosity is extremely simple and rapid and it is suitable for calibration optimization. Moreover, the quasi-linear

reverse correlation observed between porosity and not normalized analytical totals showed that these last can be used as a relative estimate of the sample porosity, as suggested by Freestone. This observation shows that when an evaluation of the porosity with the suggested method is not possible (i.e. in the case of XRF measurement without any previous microscopic morphological examination), an alternative to broadly choose the most appropriate standard is to estimate the porosity as complementary to 100% of the obtained analytical total. However, this procedure should be considered with extreme caution since this porosity assessment is more imprecise and would entail a risk of circularity if analytical totals are affected by poor accuracy.

The comparison between the two methods of sample pre-treatment revealed that powder pressing is an adequate procedure and that kneading the powders with water to simulate a clayey mixture is not necessary.

The influence of the porosity is definitely less important in the case of high temperature fired samples, such as porcelain, since porosity is low and its effect is negligible. No substantial differences were observed comparing the calibration results obtained with the ceramic standard fired at 1200°C with those pertaining to mineral/massive oxides and/or glass standards, indicating that in the case of porcelain the use of a specifically prepared standard is non influential and that the usual calibration with glasses and/or massive oxides and minerals is proper. On the other hand, the use of a standard simply obtained by pressing a powder without any subsequent firing step is unsuitable, whatever the analyzed material.

An open question is relative to the results obtained for Ca for both the considered certified standards. Ca is an important element in the characterization of ceramic and porcelain materials because it is often distinctive of specific productions and it highly influences the sample microstructure. In the present study Ca showed the highest accuracy fluctuations for both standards; this tendency was not elucidated so far but it has to be deeper evaluated analyzing more calcareous standards. Moreover, a further in-depth analysis in the case of XRF should consist

in preparing ceramic standards of different composition and to perform a calibration using this set, instead of using only one standard. Finally, additional developments should be the evaluation of the porosity influence on the XRF determination of trace elements and the comparison of the results with the corresponding data obtained by a portable XRF instrument.

The proposed calibration method seems particularly suitable for studies on production technologies or in the SEM-EDS examination of multilayer ceramics, where trends in the composition of each layer (i.e. body, slip, glaze) need to be evaluated. Moreover, it seems seminal in the case of characterization studies, in particular when data are submitted to clustering techniques. In all these cases a considerable error in the determination of the major elements would lead to erroneous conclusions.

As conclusive and general remark we would like to stress that the porosity assessment and use of opportunely prepared standard is not only relevant in calibrating the instruments, but also in assessing instrument performance and determine method suitability, when porous materials are examined. Similar chemical composition between standards and samples is not the only parameter to consider, the physical structure of the matrix is also relevant and should be take into account.

REFERENCES

Casadio, F., Bezur, A., 2009. A scientific evaluation of the materials, in: Fired by Passion. Vienna Baroque Porcelain of Claudius Innocentius Du Paquier. Arnoldsche Art Publishers, Stuttgart, pp. 1165–1203.

Correia, S.L., Hotza, D., Segadães, A.M., 2007. Predicting porosity content in triaxial porcelain bodies as a function of raw materials contents. J. Mater. Sci. 43, 696–701. doi:10.1007/s10853-007-2188-3

Davit, P., Turco, F., Coluccia, S., Operti, L., Chelazzi, F., Bombardieri, L., 2014. Technological and compositional characterization of red polished ware from the bronze age kouris valley (Cyprus). Mediterr. Archaeol. Archaeom. 14, 1–18.

Freestone, I.C., 1982. Application and potential of Electron Probe Micro-Analysis in technological and provenance investigations of ancient ceramics. Archaeometry 24, 99–116.

Freestone, I.C., Joyner, L., Howard, R., 2003. The Composition of Porcelain from the Isleworth Manufactory. English Ceram. Circ. Trans. 18, 284–293.

Goldstein, J.I., Newbury, D.E., Echlin, P., Joy, D.C., Romig, A.D.J., Lyman, C.E., Fiori, C., Lifshin, E., 1992. Scanning Electron Microscopy and X-ray Microanalysis, 2nd Edition. Plenum Press, New York.

Knížek, K., Jurek, K., 1994. Correction Procedure for the Electron Microprobe Analysis of Porous Materials. Mikrochim. Acta 117, 87–93.

Liritzis, I., Mavrikis, D., Zacharias, N., Sakalis, A., Tsirliganis, N., Polymeris, G.S., 2011. Potassium Determinations Using Sem , Faas and Xrf : Some Experimental Notes. Mediterr. Archaeol. Archaeom. 11, 169–179.

Lucas-Tooth, J., Pyne, C., 1963. The accurate determination of major constituents by X-ray fluorescent analysis in the presence of large interelement effects. Adv. X-ray Anal. 7, 523–541.

Maniatis, Y., Tite, M.S., 1981. Technological examination of Neolithic-Bronze Age pottery from central and southeast Europe and from the Near East. J. Archaeol. Sci. 8, 59–76. doi:10.1016/0305-4403(81)90012-1

Metrich, N., Clocchiatti, R., 1989. Melt inclusion investigation of the volatile behaviour in historic alkali basaltic magmas of Etna. Bull. Volcanol. 51, 185–198. doi:10.1007/BF01067955

Mirti, P., 2000. X-ray microanalysis discloses the secrets of ancient Greek and Roman potters. XRay

Spectrom. 29, 63–72. doi:10.1002/(sici)1097-4539(200001/02)29:1<63::aid-xrs409>3.0.co;2-f

Mirti, P., Davit, P., 2001. Technological Characterization of Campanian Pottery of Type A, B and C and of Regional Products from Ancient Calabria (Southern Italy). Archaeometry 43, 19–33.

Montana, G., Tsantini, E., Randazzo, L., Burgio, A., 2013. Sem-Eds Analysis As a Rapid Tool for Distinguishing Campanian a Ware and Sicilian Imitations. Archaeometry 55, 591–608. doi:10.1111/j.1475-4754.2012.00723.x

Moropoulou, A., Bakolas, A., Bisbikou, K., 1995. Thermal analysis as a method of characterizing ancient ceramic technologies. Thermochim. Acta 269–270, 743–753.

Musílek, L., Cechák, T., Trojek, T., 2012. X-ray fluorescence in investigations of cultural relics and archaeological finds. Appl. Radiat. Isot. 70, 1193–202. doi:10.1016/j.apradiso.2011.10.014

Newbury, D.E., Ritchie, N.W.M., 2013. Is Scanning Electron Microscopy/Energy Dispersive X-ray Spectrometry (SEM/EDS) Quantitative? Scanning 35, 141–168. doi:10.1002/sca.21041

Özçatal, M., Yaygıngöl, M., İssi, A., Kara, A., Turan, S., Okyar, F., Pfeiffer Taş, Ş., Nastova, I., Grupče, O., Minčeva-Šukarova, B., 2014. Characterization of lead glazed potteries from Smyrna (İzmir/Turkey) using multiple analytical techniques; Part II: Body. Ceram. Int. 40, 2153–2160. doi:10.1016/j.ceramint.2013.07.132

Papageorgiou, I., Liritzis, I., 2007. Multivariate Mixture of Normals With Unknown Number of Components: an Application To Cluster Neolithic Ceramics From Aegean and Asia Minor Using Portable Xrf. Archaeometry 49, 795–813. doi:10.1111/j.1475-4754.2007.00336.x

Seetha, D., Velraj, G., 2015. Spectroscopic and Statistical Approach of Archaeological Artifacts Recently Excavated From Tamilnadu, South India. Spectrochim. Acta Part A Mol. Biomol. Spectrosc. 149, 59–68. doi:10.1016/j.saa.2015.04.041

Shackley, M.S., 2011. An Introduction to X-Ray Fluorescence (XRF) Analysis in Archaeology, in: Shackley, M.S. (Ed.), X-Ray Fluorescence Spectrometry (XRF) in Geoarchaeology. Springer,

Springer New York. doi:10.1007/978-1-4419-6886-9

Ting, C., Martinón-Torres, M., Graham, E., Helmke, C., 2015. The production and exchange of moulded-carved ceramics and the “Maya Collapse.” J. Archaeol. Sci. 62, 15–26. doi:10.1016/j.jas.2015.06.013

Tite, M., Watson, O., Pradell, T., Matin, M., Molina, G., Domoney, K., Bouquillon, A., 2015. Revisiting the beginnings of tin-opacified Islamic glazes. J. Archaeol. Sci. 57, 80–91. doi:10.1016/j.jas.2015.02.005

Tite, M.S., 2008. Ceramic Production, Provenance and Use—a Review. Archaeometry 50, 216–231. doi:10.1111/j.1475-4754.2008.00391.x

Tite, M.S., Bimson, M., 1991. A Technological Study of English Porcelains. Archaeometry 33, 3–27. doi:10.1111/j.1475-4754.1991.tb00682.x

Turco, F., Davit, P., Maritano, C., Operti, L., Fenoglio, G., Agostino, A., 2015. XRF Characterization Of 18th Century Piedmontese Porcelains From The Palazzo Madama Museum (Torino, Italy). Archaeometry n/a-n/a. doi:10.1111/arcm.12186

Vaggelli, G., Olmi, F., Conticelli, S., 1999. Quantitative electron microprobe analysis of reference silicate mineral and glass samples. Acta Vulcanol. 11, 297–304.

Yan, L.T., Feng, S.L., Li, L., Ma, B., Liu, L., Feng, X.Q., 2015. The Compositional study of ceramic samples from tombs dating to the Zhou Dynasty at Xiaoshan, Zhejiang Province (China). Archaeometry 57, 822–836. doi:10.1111/arcm.12136

Yin, M., Rehren, T., Zheng, J., 2011. The earliest high-fired glazed ceramics in China: the composition of the proto-porcelain from Zhejiang during the Shang and Zhou periods (c. 1700–221 BC). J. Archaeol. Sci. 38, 2352–2365. doi:10.1016/j.jas.2011.04.014